Parity nonconservation in the hydrogen atom. II

R. W. Dunford,* R. R. Lewis, and W. L. Williams

Harrison M. Randall Laboratory of Physics, University of Michigan, Ann Arbor, Michigan 48109

(Received 13 June 1977; revised manuscript received 16 June 1978)

We give a complete phenomenological analysis of parity mixing in the hydrogen atom, showing the connection between relativistic neutral-current interactions and nonrelativistic potentials. The matrix elements of these potentials are evaluated for $n = 2$ hydrogen, and the mixing of $2S$-$2P$ states is computed at each of the level crossings. A systematic discussion of the invariant decomposition of $2S$-$2S'$ microwave transitions is given, providing a catalogue of the possible parity experiments. One particular transition is analyzed to show its sensitivity to weak interactions. We conclude that it should be possible to detect weak interactions of universal strength by observing asymmetries of order 10^{-6}, with integration times of order 10^4 sec. Such experiments are underway at this laboratory.

I. INTRODUCTION

The hydrogen atom has been called "the Rosetta stone of physics," because the analysis of its spectrum has played such an important role in the development of quantum theory and quantum electrodynamics.[1] It offers unique advantages for the study of small corrections to the dominant Coulomb interaction between the electron and the proton because of the accuracy with which one can solve two-body systems and because of the accidental degeneracy of its spectrum. It is natural to ask whether the hydrogen atom can also play a significant role in the search for weak interactions between electrons and nucleons. In this paper we will provide systematic answers to such questions as: what are the perturbations caused by parity nonconserving weak interactions in the hydrogen atom, what can be learned about the coupling constants, and how can one enhance the very small effects of weak parity mixing? We will show that the high precision of the theory of atomic hydrogen is indeed a major advantage in predicting, and eventually analyzing, parity nonconserving effects and that additional "accidental" features are an aid in the search for these effects.

We have already provided some answers to these questions in an earlier publication.[2,3] We showed that $2S$-$2P$ level crossings serve both to enhance the parity mixing, and to provide a natural separation of the nuclear spin-independent and spin-dependent terms. Two different parity nonconserving effects were analyzed. One of these, circular dichroism in the optical transition $2S \rightarrow 3S$, employs a classical optical technique for the determination of handedness. The other, which has no classical analog, involves the quench probability of a $2S$ atom in parallel static $\vec{E}$ and $\vec{B}$ fields. We concluded that a realistic

appraisal of various experimental parameters showed that weak interactions of universal strength could be observed with integration times of about one day.

This paper has a similar organization and provides a more detailed analysis of related questions. In Sec. II we will review earlier theoretical and experimental results pertaining to parity conservation in hydrogen. In Sec. III we will give a complete tabulation of parity mixing in $n = 2$ atomic hydrogen, with emphasis on the level crossings. It will be shown that there are three different weak potentials giving parity mixing amplitudes of the same order of magnitude, and that there is a clear separation of these potentials at different level crossings. In Sec. IV we will give a systematic classification of all the scalar and pseudoscalar terms which can arise for microwave transitions within the $n = 2$ shell. In Sec. V, we will discuss a particular microwave transition and show that it can be made to give a larger parity nonconserving asymmetry than either optical transitions or quenching in static fields.

As will be discussed in Sec. II, several authors have already emphasized the special advantages of the hydrogen atom, but have shown that parity mixing should occur with very small amplitude, many orders of magnitude smaller than existing experimental limits. On the other hand, it has been argued that parity mixing between S and P states in heavy atoms should occur with a size which is accessible in experiments using available laser technology.[4] Our purpose here is to show that parity conservation in hydrogen can also be tested down to the level at which an effect is expected. This is intended to emphasize that parity mixing in one-electron atoms should be observable, and can provide a complete determination of the coupling constants. Our work goes

beyond just tabulating the parity mixing effects between various states in hydrogen, and presents a discussion of the general ideas of designing parity experiments. We have arbitrarily limited the scope of this discussion to hydrogen, and to the atomic physics aspects of these calculations. We have stopped short of a detailed description of any specific experiment. An experimental program is in progress at this laboratory, and results will be presented at a later time.

II. REVIEW OF PARITY NONCONSERVATION IN ATOMIC HYDROGEN

The possibility that there are weak interactions of the form

$$H_W = \frac{1}{\sqrt{2}} G \int d^3x (\bar{e}0e)(\bar{p}0p), \tag{1}$$

between electron proton and electron neutron, where G is the Fermi constant, has been conjectured by many people in the past. The first specific consideration of parity nonconservation in weak interactions of this type was apparently due to Zel'dovich,[5] who discussed several consequences of putting $0 = \gamma_\mu (1 + \gamma_5)$ in Eq. (1). In atomic hydrogen, this leads to a mixing of the closely spaced levels $2S_{1/2}$ and $2P_{1/2}$ with matrix element

$$(2P_{1/2}|H_W|2S_{1/2}) = +i \frac{\sqrt{3}}{32\pi\sqrt{2}} \left(\frac{G\alpha}{a_0^3} \right). \tag{2}$$

As could be expected, the matrix element is of order G/(atomic volume); no dependence on nuclear spin (hyperfine effect) has been included. The extra power of $\alpha \cong \frac{1}{137}$ comes from the evaluation of the $2P$ amplitude at the nucleus, which arises only from keeping first-order relativistic corrections. Combining this with the energy separation (Lamb-shift)

$$E(2S_{1/2}) - E(2P_{1/2}) \cong 0.414\alpha^5 mc^2, \tag{3}$$

leads to a mixing amplitude

$$\delta_W = \frac{(2P_{1/2}|H_W|2S_{1/2})}{E(2S) - E(2P)} = +i(0.029)G \left(\frac{mc}{e\hbar} \right)^2$$

$$\approx +i \times 10^{-11}. \tag{4}$$

Zel'dovich noted that this mixing would result in a weak-induced electric dipole amplitude for the decay $2S \rightarrow 1S$, but that this amplitude would be smaller than the spontaneous magnetic dipole amplitude, and would make an unobservable change in the decay rate of the metastable $2S$ state. He also considered the optical activity which would arise from the interference of the magnetic dipole and the electric dipole amplitudes. This effect would be linear in G rather

than quadratic, and more sensitive to weak interactions. Again he found a very small effect, apparently offering no hope of detection.

Michel carried the analysis of such neutral currents further,[6] writing out the parity nonconserving electron-nucleon potentials for a particular model. He recognized the advantage of causing the $2S$-$2P$ levels to cross in a magnetic field $\vec{B}$, which would increase the mixing amplitude by a factor $[E(2S) - E(2P)]/\frac{1}{2}\hbar\Gamma_{2P} \cong 21$, Γ_{2P} being the natural decay rate of the $2P$ state. He also emphasized that motional electric fields $\vec{v} \times \vec{B}/c$ would produce mixing of these same states, putting stringent requirements on the collimation of velocity in any metastable beam experiment.

Michel suggested another effect linear in G, involving the circular dichroism (CD) of the microwave transition $2P_{3/2} \rightarrow 2P_{1/2}$. This transition has a magnetic dipole amplitude

$$M1 = \mu_0(2P_{1/2}|\sigma_z + L_z|2P_{3/2}) = \sqrt{2}\,\mu_0/3 \tag{5}$$

and a weak-induced electric dipole amplitude

$$E1_W = \delta_W(2S_{1/2}|ez|2P_{3/2}) = \sqrt{6}\,\delta_W ea_0. \tag{6}$$

The resultant CD would be

$$CD = |2\delta(E1/M1)| = 12\sqrt{3}\,|\delta|/\alpha \approx 10^{-8}. \tag{7}$$

This was the first suggestion of a parity experiment which would enhance the contribution of weak interactions, in this case by the factor $(E1/M1) = 6\sqrt{3}/\alpha = 1424$. The experiment is not practical with thermal energy beams, however, since the transition is between unstable states which decay in a distance of order 10^{-3} cm, much smaller than the wavelength of the microwaves.

On the experimental side, Fite et al. have measured the Lyman-α radiation from a metastable hydrogen beam, arising primarily from collision-induced emission.[7] The residual radiation *not* associated with collisions sets an upper limit on the spontaneous rate of one photon transitions $2S \rightarrow 1S$. Their limit gives an upper bound to the parity mixture at zero magnetic field

$$|\delta(H)| \leq 8 \times 10^{-4}. \tag{8}$$

This limits both the nuclear spin-independent and spin-dependent contributions, but with bounds much higher than the results expected from weak interactions.

Robiscoe has improved on this limit using the enhanced mixing in a magnetic field, by studying the quenching of a metastable hydrogen beam in a magnetic field of 538 G, where a $2S$-$2P$ crossing occurs.[8] At this particular level crossing, the parity mixing occurs between states arising from different F values, which has been shown to single

out the contributions of the nuclear spin-dependent part of the weak interaction.[2] The upper bound deduced from this measurement was

$$|\delta(H)| \leqslant 9 \times 10^{-5}. \tag{9}$$

More recently, the $2S \to 1S$ one photon transition has been observed in the hydrogenic ion A^{17+} by Marrus and Schmieder.[9] The calculated $M1$ rate rises very rapidly with Z, becoming the dominant decay mechanism in heavier ions. The calculated rate is compatible with the observed rate, setting an upper bound on the square of the weak-induced $E1$ amplitude. This leads to a bound on the mixing parameter

$$|\delta(A)| \leqslant 6 \times 10^{-4}, \tag{10}$$

which is also much bigger than what is expected from weak interactions. Feinberg and Chen[10] have calculated the Z-dependence of this parameter as a by-product of their work on parity non-conservation in muonic atoms; it increases somewhat faster than Z.

The largest effect predicted to this date comes from the circular polarization or anisotropy of the one photon transition, $2S \to 1S$ in hydrogen. Moskalev has shown that the weak-induced $E1$ amplitude competes very favorably with the $M1$ amplitude, which is strongly suppressed in transitions between different shells.[11] The parity mixture in $2S$ is enhanced by a factor

$$E1/M1 = (1S|ez|2P)/(1S|\mu_0\sigma_z|2S) = 2^6/9\sqrt{3}\,\alpha^3$$
$$= 1.06 \times 10^7, \tag{11}$$

giving a polarization and anisotropy of order 10^{-4}. This enhancement is somewhat illusory, however, since the strong suppression of $M1$ makes this a very rare decay mode. The large asymmetry is accompanied by a very low event rate, and is an advantage to the experiment only if background contributions to the rate, such as collision induced decays, can be kept as small as the spontaneous decay rate. The observation of this polarization seems hopeless, since suitable circular polarimeters are not available at this wavelength (vacuum uv); however, measuring the anisotropy may be a viable experiment with heavy hydrogenic ions.

To summarize this brief review, it is clear that the existing experimental evidence for parity conservation in one-electron atoms is much too insensitive to draw any conclusion about weak interactions of universal strength G. This results largely from the absence of any experiment sensitive to interference effects of order G, rather than rates of order G^2. Although several such experiments have been suggested, the theoretical

work has concentrated on processes that lack practical feasibility. There is a need for a more systematic tabulation of parity nonconserving effects in hydrogen, and a more realistic assessment of the experimental realities. That is the task which we set ourselves in the next sections.

III. PARITY MIXING IN $n=2$ HYDROGEN

Gauge theories of weak and electromagnetic interactions offer the hope of unifying these interactions into a single theoretical framework which permits the calculation of processes involving leptons and hadrons, in our case electrons and nucleons, to any desired accuracy, free of divergent integrals and arbitrary constants. At the moment, such theories have not been refined to the point where, like quantum electrodynamics, one is confident of the structure of the theory and the values of the coupling constants. On the contrary, it is not yet certain whether neutral currents of electrons participate in weak interactions, and have both vector and axial vector parts. It has not yet been established what the gauge group is, what assignment of particle multiplets is correct and what the mixing angles are. In this situation, we feel that the first task in analyzing parity nonconservation is to make an empirical approach, without reference to any particular gauge model. This puts the burden of the determination of the coupling constants on the experiments, as a guide to a specific choice of model.

The reasonable goals of parity experiments in hydrogen are to observe an unambiguous effect of weak interactions, and to measure its strength to (say) 10% precision. Only in the distant future can one foresee measurements of parity mixtures with enough precision to measure relativistic and radiative corrections[12] of order $v/c \simeq \alpha \simeq 10^{-2}$, or recoil corrections of order $m/M \simeq 10^{-3}$. Our goal therefore is to analyze parity mixtures to leading order in α and m/M. We begin the discussion by considering the general form of a nonrelativistic potential describing the parity nonconserving part of the energy of an electron in the vicinity of a stationary nucleus. This potential is to be used with gross structure eigenstates. This will provide the most direct link between experimental information and model calculations.

A. Nonrelativistic parity-nonconserving potential

The form of a parity-nonconserving potential is restricted by the general features of weak interactions. We assume Hermiticity and Galilean relativity, and retain only the P-odd (pseudoscalar) terms. We also assume the range of weak

interactions to be very short compared with atomic dimensions, and therefore choose a potential having delta function dependence on the electron-nuclear separation $\vec{r}$. The dependence on the relative momentum $\vec{p}$ will be treated by a series expansion in powers of p/mc. Since successive terms are of order $(p/mc) \simeq \alpha$, we need keep only the leading term.

T-invariance is the only remaining general principle which might be applied. There already exists experimental evidence, derived from the absence of linear Stark shifts in the levels of heavy atoms and molecules, that P-odd T-odd weak interactions must have coupling constants smaller than about 10^{-3} G.[13] The parity experiments under discussion in hydrogen do depend on T-odd as well as T-even terms. However they are not sensitive to terms as small as 10^{-3} G, and so in the remainder of our treatment, T invariance will be assumed. There may be a point to setting limits on the T-odd contributions in a simple atom such as hydrogen, but we will not consider that possibility here.

The parity nonconserving electron-proton potential contains *no* terms independent of momentum. Under the assumptions listed above, the only pseudoscalars independent of $\vec{p}$ are $\vec{\sigma}_1 \cdot \vec{r}\delta(\vec{r})$ and $\vec{\sigma}_2 \cdot \vec{r}\delta(\vec{r})$, which vanish identically. Here $\vec{\sigma}_1$ is the electron spin and $\vec{\sigma}_2$ the proton spin. In the next order of $\vec{p}/m$ there are *three* independent pseudoscalars $\vec{\sigma}_1 \cdot \vec{p}\delta(\vec{r})$, $\vec{\sigma}_2 \cdot \vec{p}\delta(\vec{r})$ and $\vec{\sigma}_1 \times \vec{\sigma}_2 \cdot \vec{p}\delta(\vec{r})$. The resulting hermitian potential can conveniently be parametrized as

$$V = \frac{G}{\sqrt{8}\,mc}\{-C_{1p}[\vec{\sigma}_1 \cdot \vec{p}, \delta(\vec{r})]_+ + C_{2p}[\vec{\sigma}_2 \cdot \vec{p}, \delta(\vec{r})]_+$$
$$- i(C_{2p} + C_{3p})[\vec{\sigma}_1 \times \vec{\sigma}_2 \cdot \vec{p}, \delta(\vec{r})]_-\},$$

(12)

where $[A, B]_\mp$ denotes the commutator, anticommutator. A dimensional constant $G/\sqrt{8}\,mc$ has been factored out. The remaining quantities C_{1p}, C_{2p}, and C_{3p} are real dimensionless parameters, presumably of order unity, the only unknown quantities in our potential. The same form can be used for the electron-neutron potential, with C_{1n}, C_{2n}, and C_{3n} instead. The terms containing C_2 can be rewritten in the alternative form

$$V_2 = +(GC_{2p}/\sqrt{8}\,mc)[\vec{\sigma}_1 \cdot \vec{p}\,\vec{\sigma}_1 \cdot \vec{\sigma}_2\delta(\vec{r}) + \text{H.c.}].$$

(13)

Our choice of constants may look a bit strange at this point, but will be seen to be appropriate when we discuss the connection with the relativistic interactions from which they arise, and when we evaluate parity mixing at the level crossings.

Inspection of the potentials in Eq. (12) reveals the selection rules governing their matrix elements. The $\delta(\vec{r})$, $\delta'(\vec{r})$ singularity restricts the orbital angular momentum to $l = 0$ and 1, which correspond to the only states having a finite value or derivative at the nucleus. The asymmetry under spatial inversions implies that they only connect S and P states. The potential V_1, defined by the coefficient of C_1, is independent of the nucleon spin and therefore preserves $\vec{I}$ and $\vec{J}$ but can flip $\vec{L}$ and $\vec{S}$ ($\Delta m_l = 0, \pm 1; \Delta m_s = 0 \pm 1$). The other two potentials, V_2 and V_3, preserve only $\vec{F} = \vec{L} + \vec{S} + \vec{I}$ and can flip the individual angular momenta $\vec{L}$, $\vec{S}$, $\vec{I}$. We will see the implications of these selection rules at the various level crossings below.

B. Relativistic interaction of neutral currents

The description of this weak interaction can also be given in terms of the local coupling of two Lorentz-covariant neutral currents. The hadron current will be expressed in terms of the nucleon content rather than in terms of its quark content. If we use a similar set of assumptions (Hermiticity, Lorentz invariance, T invariance, P nonconservation) then it is reasonable to expect the same number of parameters, and to recover the same potentials in the nonrelativistic reduction. The only thing to be learned from this reduction is the relationship between the parameters C_1, C_2, C_3 and the form factors of the currents.

We introduce a vector current V_μ and an axial-vector current A_μ for both the electron and the nucleon. According to well known arguments,[14] the matrix elements of the electron current between free in-out states have the following general form,

$$\langle p'| V_\mu^e |p\rangle = i\bar{u}(p')[f_1^e\gamma_\mu + f_2^e q_\nu\sigma_{\nu\mu}]u(p),$$
$$\langle p'| A_\mu^e |p\rangle = i\bar{u}(p')[g_1^e\gamma_5\gamma_\mu - g_2^e q_\mu\gamma_5]u(p),$$

(14)

where f_1, $2mf_2$, g_1, and $2mg_2$ are called, respectively, the "weak charge," the "weak anomalous moment," the "axial charge," and the "induced pseudoscalar" form factors of the electron. They will be considered as constants for the low momenta in atoms. The terms containing $q_\mu = p'_\mu - p_\mu$ have been normalized by a factor $(2m)^{-1}$ using the electron mass. Since we are interested in analyzing experimental results without any further theoretical input, we shall include on an equal footing both the "intrinsic" form factors f_1^e, g_1^e and the "induced" terms f_2^e, g_2^e.

We can use the same general form of (14) for the proton and the neutron, with appropriate changes in the superscripts, and with replacement of the electron mass m by the nucleon mass M.

The parity nonconserving semileptonic interaction arising from the local coupling of those two currents will be

$$H_{\text{weak}} = \frac{1}{\sqrt{2}} G \int d^3x (A^e_\mu V^p_\mu + V^e_\mu A^p_\mu)$$

$$= \frac{1}{\sqrt{2}} G \int d^3x \{ [i\, g^e_1(\bar{e}\gamma_5\gamma_\mu e) + g^e_2 \partial_\mu(\bar{e}\gamma_5 e)][if^p_1(\bar{p}\gamma_\mu p) - f^p_2 \partial_\nu(\bar{p}\sigma_{\nu\mu} p)]$$

$$+ [if^e_1(\bar{e}\gamma_\mu e) - f^e_2 \partial_\nu(\bar{e}\sigma_{\nu\mu} e)][i\, g^p_1(\bar{p}\gamma_5\gamma_\mu p) + g^p_2 \partial_\mu(\bar{e}\gamma_5 e)] \} , \tag{15}$$

which superficially appears to contain eight terms. However, the contributions of "induced pseudoscalar" (g_2) terms vanish identically since they can be integrated by parts to give the divergence of currents which are conserved,

$$\partial_\mu \bar{\psi}\gamma_\mu\psi = 0 , \quad \partial_\mu \partial_\nu \bar{\psi}\sigma_{\mu\nu}\psi = 0 . \tag{16}$$

This remains valid even for electrons bound by a static potential. The contributions of the nucleon "anomalous moment" (f_2) terms can also be discarded as negligibly small, since they are reduced by a factor $p/Mc \approx \alpha(m/M)$. The remaining terms give three interactions[15]

$$H_W = \frac{1}{\sqrt{2}} G \int d^3x [g^e_1 f^p_1(\bar{e}\gamma_\mu\gamma_5 e)(\bar{p}\gamma_\mu p)$$

$$+ f^e_1 g^p_1(\bar{e}\gamma_\mu e)(\bar{p}\gamma_\mu\gamma_5 p)$$

$$+ if^e_2 g^p_1 \partial_\nu(\bar{e}\sigma_{\nu\mu} e)(\bar{p}\gamma_\mu\gamma_5 p)] . \tag{17}$$

A nonrelativistic reduction of Eq. (17) can be seen to reproduce the potential of Eq. (12), with the following identification of constants

$$C_{1p} = g^e_1 f^p_1 , \quad C_{2p} = f^e_1 g^p_1 , \quad C_{3p} = f^e_2 g^p_1 . \tag{18}$$

This justifies our selection of the particular form of Eq. (12). The terms containing C_1, C_2 arise from the "weak charge" and the "weak axial charge" of the electron and nucleon. Measurement of these quantities for both the proton and neutron are the goals of this research; they would provide basic constants of importance to the theory of weak interactions, and would help to discriminate among the many models already proposed.[16]

The terms containing C_1 have attracted the most attention, since they may be enhanced in heavy atoms by the coherent superposition of many nucleons. The terms containing C_2 depend on the nucleon spin and are not enhanced in heavy atoms. They may be detectable there if the experimental sensitivity is sufficiently high, but are comparable in strength with radiative corrections to C_1 and will be difficult to differentiate. The values of these constants predicted by a variety of gauge models are given in Ref. 16. Our parametrization of the potential V [Eq. (12)] facilitates the direct comparison of experimental results with quark model results.

The terms containing C_3 have received little attention. If we assume that the only neutral vector current is the electromagnetic current, then the form factors are known and C_3 is small. Neglecting radiative and binding corrections, we have

$$C_{3p}/C_{2p} = f^e_2/f^e_1 \cong \alpha/2\pi + \cdots \ll 1 . \tag{19}$$

However, we feel that it is important at this time to provide an empirical test of such results and to verify experimentally whether the electron vector current does in fact have the same structure as the electromagnetic current. We will therefore retain C_3 as a parameter of order unity and discuss the problem of extracting this constant along with C_1 and C_2 from experiment.

C. Weak interaction matrix elements

Next we consider the matrix elements of the weak potential V in Eq. (12). Figure 1 shows the Zeeman diagram for $n = 2$ hydrogen, with the states labeled in the notation of Lamb and Retherford.[17] Level crossings are seen to occur for magnetic fields between 500 and 7500 G. The representation of the bound states will be chosen to simplify the calculation of parity mixing at the various crossings. In this region, the energy eigenstates are mixed by the combined effects of spin-orbit, hyperfine, and Zeeman interactions. For most of this range of magnetic fields, these energies are ordered according to

$$H_{\text{hfs}} < H_{\text{Zeeman}} < H_{\text{spin/orbit}} , \tag{20}$$

where hfs stands for hyperfine structure. This implies that the electron spin and orbital angular momenta are strongly coupled and oriented by the magnetic field, but that they are decoupled from the nuclear spin. The most appropriate representation is therefore $|LSJm_J Im_I\rangle$. At the first level crossing ($B \simeq 538$ G) the mixing of states with different m_J, m_I by the hyperfine interaction is less than 6% in amplitude; at the last level crossing ($B \simeq 7081$ G) the mixing of states of different J by the Zeeman interaction is about 43% in amplitude. These mixing effects will be included in
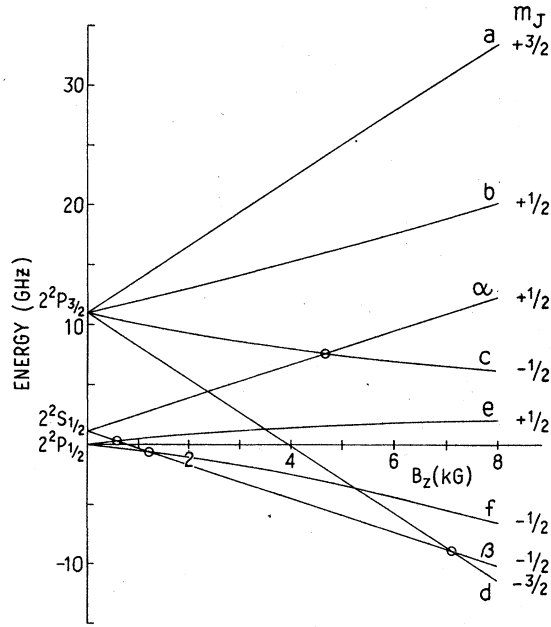
FIG. 1. Zeeman diagram for hydrogen, showing the level crossings (the circles) at which parity mixtures can occur. The states are labeled using Lamb's nomenclature, and the intermediate field quantum numbers shown. The hyperfine structure is not included in this diagram.

our numerical calculations, and are mentioned here only to explain our choice of basis and to indicate the general scale of the mixing.

Having chosen the basis, we must also carefully specify the relative phases of the states since they govern the phases of various amplitudes. We have found it useful for many purposes to construct the basis states explicitly by using various operators on the $S_{1/2}$ states. We choose the following states,[18]

$$|nS_{1/2}, m_J = \pm \tfrac{1}{2}, m_I\rangle = \frac{1}{\sqrt{4\pi}} R_{n0}(r)\chi_{1/2}^{m_J}\chi_I^{m_I}$$

$$|nP_{1/2}, m_J = \pm \tfrac{1}{2}, m_I\rangle = -\frac{1}{\sqrt{4\pi}} \frac{R_{n1}(r)}{r} \vec{\sigma}_e \cdot \vec{r}\chi_{1/2}^{m_J}\chi_I^{m_I}$$

$$|nP_{3/2}, m_J = \pm \tfrac{1}{2}, m_I\rangle = \pm \frac{1}{\sqrt{8\pi}} \frac{R_{n1}(r)}{r} (3\sigma_{ez}z - \vec{\sigma}_e \cdot \vec{r})\chi_{1/2}^{m_J}\chi_I^{m_I}$$

$$|nP_{3/2}, m_J = \pm \tfrac{3}{2}, m_I\rangle = \mp \left(\frac{3}{8\pi}\right)^{1/2} \frac{R_{n1}(r)}{r} (x \pm iy)\chi_{1/2}^{m_J \mp 1}\chi_I^{m_I}.$$

$$(21)$$

The matrix elements of V can be evaluated by integration of these wave functions over the electronic variables, leaving the nuclear variables to be evaluated separately. The nuclear matrix elements are of two types, either independent of, or containing the nucleon spins. To simplify the

presentation, we introduce the following notation for these nuclear matrix elements, which is based on the Wigner-Eckart theorem,

$$C_1 \equiv \frac{1}{2}\sum_j (\text{Im}_I'|C_{1p}(1 + \tau_{3j}) + C_{1n}(1 - \tau_{3j})|\text{Im}_I)$$

$$= ZC_{1p} + NC_{1n}$$

$$C_2(\text{Im}_I' | \vec{I} | \text{Im}_I) \equiv \frac{1}{4}\sum_j \{(\text{Im}_I'|\sigma_j[C_{2p}(1 + \tau_{3j})$$

$$+ C_{2n}(1 - \tau_{3j})]|\text{Im}_I)\}$$

$$(22)$$

$$C_3(\text{Im}_I' | \vec{I} | \text{Im}_I) \equiv \frac{1}{4}\sum_j \{(\text{Im}_I'|\sigma_j[C_{3p}(1 + \tau_{3j})$$

$$+ C_{3n}(1 - \tau_{3j})]|\text{Im}_I)\}.$$

The effective coupling constant C_1 depends only on the numbers of protons and neutrons, while C_2 and C_3 are weighted averages of the nucleon spins. This notation has the simple property that for a proton

$$C_1 = C_{1p}, \quad C_2 = C_{2p}, \quad C_3 = C_{3p}, \quad (23)$$

while for the deuteron (neglecting the small admixture of ^3D state in the ^3S ground state)

$$C_1 = C_{1p} + C_{1n}, \quad C_2 = \tfrac{1}{2}(C_{2p} + C_{2n}), \quad C_3 = \tfrac{1}{2}(C_{3p} + C_{3n}).$$

$$(24)$$

With this notation, we can now express the matrix elements of V as follows:

$$(nS_{1/2}, m_J', m_I'|V|nP_{1/2}, m_J, m_I)$$

$$= +i\,\bar{V}(m_J', m_I'| - C_1 + 2(C_2 + \tfrac{2}{3}C_3)\vec{\sigma}_e \cdot \vec{I}|m_J, m_I),$$

$$(nS_{1/2}, m_J', m_I'|V|nP_{3/2}, m_J = \pm\tfrac{1}{2}, m_I)$$

$$(25)$$

$$= \pm i\frac{\sqrt{2}}{3}\bar{V}C_3(m_J', m_I'|3\sigma_{ez}I_z - \vec{\sigma}_e \cdot \vec{I}|m_J, m_I)$$

$$(nS_{1/2}, m_J', m_I'|V|nP_{3/2}, m_J = \pm\tfrac{3}{2}, m_I)$$

$$= -i(\tfrac{2}{3})^{1/2}\bar{V}C_3(m_J', m_I'|\sigma_{ez}(I_x \pm iI_y)|m_J \mp 1, m_I).$$

The magnitude of these matrix elements are governed by the dimensional factor $\bar{V}$, defined by

$$\bar{V} \equiv \frac{3G}{8\pi\sqrt{2}} R_{n0}(0)R_{n1}'(0)\left(\frac{\hbar}{mc}\right) = \frac{G\alpha Z^4}{2\pi\sqrt{2}\,a_0^3}\frac{\sqrt{n^2-1}}{n^4}$$

$$= 0.118 Z^4 \frac{\sqrt{n^2-1}}{n^4}\,\text{Hz}.$$

$$(26)$$

We also list the matrix elements of the Stark interaction $\Phi = e\vec{E}\cdot\vec{r}$ in this same basis,

$$(nS_{1/2}m'_J m'_I|\Phi|nP_{1/2}m_J m_I) = -\overline{\Phi}\delta_{m'_I m_I}(m'_J|\vec{\sigma}_e \cdot \hat{E}|m_J),$$

$$(nS_{1/2}m'_J m'_I|\Phi|nP_{3/2}m_J = \pm \tfrac{1}{2}, m_I)$$

$$= \pm \frac{1}{\sqrt{2}}\overline{\Phi}\delta_{m'_I m_I}(m'_J|3\sigma_{ez}\hat{E}_z - \vec{\sigma}_e \cdot \hat{E}|m_J), \quad (27)$$

$$(nS_{1/2}m'_J m_I|\Phi|nP_{3/2}m_J = \pm \tfrac{3}{2}, m_I)$$

$$= \mp (\tfrac{3}{2})^{1/2}\overline{\Phi}(\hat{E}_x \pm i\hat{E}_y)\delta_{m'_I m_I}\delta_{m'_J, m_J \mp 1},$$

where $\overline{\Phi}$ is the quantity

$$\overline{\Phi} = \tfrac{1}{3}eE \int_0^\infty r^3 dr R_{n0}R_{n1} = -\frac{eEa_0}{2Z}n\sqrt{n^2-1}. \quad (28)$$

These energy matrices, when added to the diagonal matrices for fine structure and Zeeman energy,[19] provide the starting point for a numerical program yielding the energy eigenvalues and eigenvectors for $n=2$ hydrogen. There is no difficulty in carrying this out to an accuracy greater than is necessary for our purpose, using either theoretical or experimental determinations of the fine structure interval, Lamb shift, and electron magnetic moment. We have chosen to calculate energies to a precision of 10 kHz, which is about ten times larger than any discrepancy between theory and experiment and at least ten times smaller than the precision required for the first parity experiments.

D. Parity mixing in $n=2$ hydrogen

We consider here the question of what parity mixing is induced by each of the terms in the weak interaction, at each of the level crossings in the $n=2$ state. This has a direct bearing on the empirical question of what could be learned about weak interactions in any specific parity experiment. Without consideration of particular details, such experiments generally involve the interference of a weak-induced parity nonconserving amplitude with a parity conserving amplitude (either a Stark-induced electric dipole amplitude, or an intrinsic magnetic dipole amplitude). Any such effect will be more easily detected by the level crossing technique,[20] since the vanishing of the real part of an energy denominator can enhance the magnitude of the weak amplitude and change its phase through π, giving a characteristic resonance line shape to the parity nonconserving effect.[21]

At each of the four level crossings in Fig. 1, shown by small circles, the value of the energy denominator at the level crossing has about the same value ($\tfrac{1}{2}i\hbar\Gamma_{2P}$, where Γ_{2P} is the natural decay rate of the $2P$ state) since each crossing represents the degeneracy of a metastable $2S$ state ($\Gamma_{2S} \simeq 0$) with an unstable $2P$ state ($\Gamma_{2P}/2\pi \cong 99.47$ MHz). Our computations show
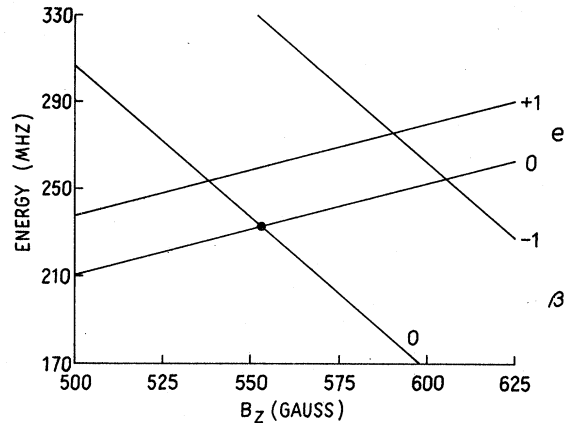

FIG. 2. States near the β-e level crossing, showing the hyperfine structure for hydrogen. The intersection of states mixed by weak interactions are indicated by a black dot.

that the energy numerators (weak matrix elements) at each of these points are also of comparable size $\langle V\rangle \simeq i\overline{V} = i(0.013$ Hz), leading to parity mixtures of order $\overline{V}/\tfrac{1}{2}\hbar\Gamma_{2P} = 2.5 \times 10^{-10}$. These factors set the general scale of parity mixing at the level crossings, and demonstrate that experiments in hydrogen have comparable sensitivity at each of the level crossings and can be expected to give comparable accuracy in the determination of the constants C_1, C_2, C_3.

The specific combination of these constants has been evaluated numerically for each of the $2S$-$2P$ level crossings circled on Fig. 1. Inspection of the enlarged diagrams in Figs. 2–5 shows that there are five pairs of $2S$-$2P$ states with the same $m_F = m_I + m_J$ which cross and can be mixed by weak interactions. We have not included the α-d crossing at 2360 G among these because no appreciable weak mixing can occur there. For the α-d states in hydrogen, there are no levels with the same m_F and so mixing is strictly forbidden by angular momentum conservation. For the α-d
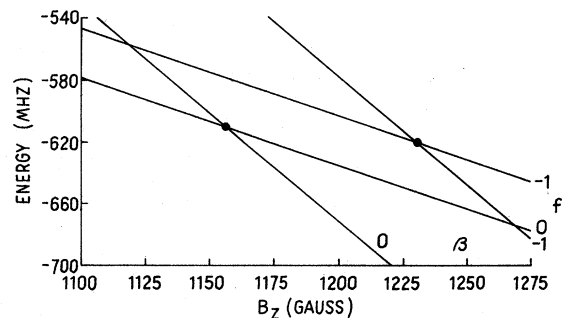

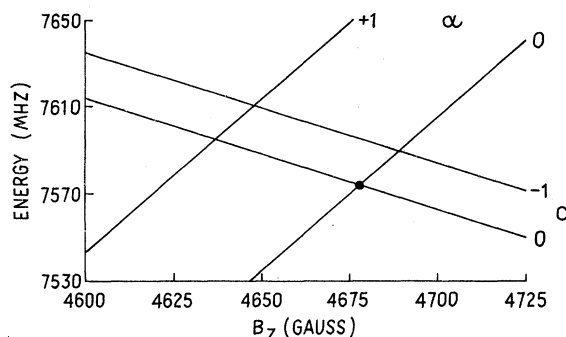FIG. 3. States near the β-f level crossing, showing the hyperfine structure for hydrogen.

FIG. 4. States near the α-c level crossing, showing the hyperfine structure for hydrogen.

states in deuterium there is one pair of states with the same m_F, but with m_J differing by 2. Mixing of these states can only come from parity nonconserving tensor forces, which occur in order $(p/mc)^2$ and are suppressed by an additional power of α.

Table I gives the weak matrix elements for each of these pairs of states, together with the magnetic field at which the crossing occurs. From these results we see that the β-e crossing is very insensitive to C_1, and determines a combination of C_2 and C_3 (approximately $C_2 + \frac{2}{3}C_3$). The β-f crossings depend on C_1 plus or minus the same combination of C_2, C_3. The high field crossings of c-α and d-β determine essentially C_2 and C_3, respectively. Thus there is a natural separation of the contributions of C_1, C_2, C_3 at the various level crossings in hydrogen. Similar results pertain to deuterium.

It is important to understand these results, rather than to simply tabulate them. The near cancellation of C_1 at the β-e crossing has been discussed earlier.[2] The states β_0 and e_0 arise out of the 2S $(F = 0)$ and 2P $(F = 1)$ states with $m_F = 0$, and have orthogonal spin wave functions at zero field. Since C_1 depends only on the numbers of nucleons and not their spins [see Eq. (22)], it cannot couple these states at zero field. As the magnetic field is increased there is mixing of the $F = 0$ and $F = 1$ states in both 2S and 2P multiplets. In fact, the magnetic mixing is almost
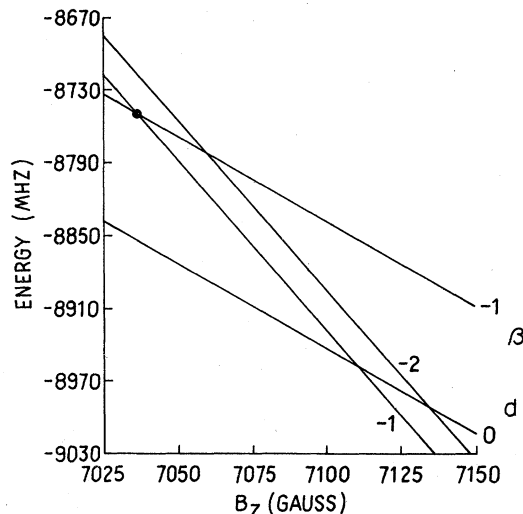

FIG. 5. States near the β-d level crossing, showing the hyperfine structure for hydrogen.

the same in these two multiplets since the magnetic moments and the hyperfine separations have about the same ratio

$$\Delta w(2S_{1/2})/\Delta w(2P_{1/2}) \cong 3 \cong g_J(2S_{1/2})/g_J(2P_{1/2}).$$

$$(29)$$

Hence, the states remain nearly orthogonal up to the level crossings; C_1 does not appreciably mix these two states at any magnetic field. This cancellation must be considered a fortuitous accident of the pure Coulomb field and the Landé formula. The implication of this accident is that parity experiments at the β-e crossing depend only on the spin dependent interactions C_2 and C_3.

By contrast, the β_0-f_0 states, both of which arise out of states with the same F at zero field, are mixed by both spin-independent (C_1) and spin-dependent (C_2, C_3) weak interactions at any field. This is also true for β_{-1}-f_{-1} mixing. The reason for the nearly opposite contributions of C_2 and C_3 at the two β-f crossings is that the states there have nearly pure m_I, m_J (Paschen-Back limit) and opposite m_I; this situation pertains at any high field $B \gg 100$ G. The implication of this is

TABLE I. Matrix elements of V for hydrogen at each of the level crossings, in units of $i\overline{V}$. The magnetic field at each crossing is also given in Gauss.

Matrix element $(i\overline{V})$		Magnetic field (Gauss)
$(e_0 \mid V \mid \beta_0)$	$= 0.00\,004C_1 - 1.98\,591C_2 - 1.31\,020C_3$	553.09
$(f_0 \mid V \mid \beta_0)$	$= 0.99\,737C_1 + 1.10\,622C_2 + 0.70\,358C_3$	1156.40
$(f_{-1} \mid V \mid \beta_{-1})$	$= 0.99\,696C_1 - 0.99\,696C_2 - 0.62\,736C_3$	1230.43
$(c_0 \mid V \mid \alpha_0)$	$= -0.00\,229C_1 + 0.60\,121C_2 - 0.05\,244C_3$	4677.83
$(d_{-1} \mid V \mid \beta_{-1})$	$= -0.00\,212C_1 + 0.00\,212C_2 - 0.81\,581C_3$	7036.43

that in any experiment at the $\beta\text{-}f$ crossing which sums over the hyperfine structure, C_2 and C_3 will nearly cancel and the experiment will be sensitive primarily to C_1.

At a field of 7036 G, there is a crossing between two states with nearly pure J, $\beta(J = \frac{1}{2})$ and $d(J = \frac{3}{2})$. Since C_3 is the only interaction which can couple $2S_{1/2}$ and $2P_{3/2}$, this crossing singles out C_3. At the other high field crossing of $\alpha\text{-}c$ at 4678 G, the magnetic mixing results in a strong cancellation of the C_3 contributions and so this crossing is sensitive primarily to C_2. The cancellation appears to be a numerical accident, and pertains only to this region of magnetic field strength. On the other hand, the vanishing of C_1 and C_2 in the $S_{1/2} - P_{3/2}$ mixing is not related to any special magnetic field, or to any property of the Coulomb field, but can be traced to the spin-angle factors in the matrix element. It should occur in any atom with the same values of L, S, and J. The implication of the cancellation of C_1 and C_2 at the $\beta\text{-}d$ crossing is that a parity experiment there can separately measure the *anomalous* part of the weak magnetic moment of the electron. This situation is reminiscent of the equality of spin and orbital precession frequencies of an electron in a uniform magnetic field, which makes possible the direct measurement of the anomaly in the magnetic moment ($g\text{-}2$ experiment).

To summarize, we see that parity mixtures resulting from weak interactions occur with roughly equal magnitude, for equal coupling strength, at various level crossings in the $n = 2$ shell of hydrogen and deuterium. Experiments at four crossings (575, 1190, 4665, and 7081 G) can provide as many as five separate data in hydrogen and nine in deuterium, giving an overconstrained fit to the six parameters of the model for any gauge theory. There is a natural separation of the effects of C_1, C_2, and C_3 with experiments at 575 G determining $C_2 + \frac{2}{3}C_3$, at 1190 G determining $C_1 \pm (C_2 + \frac{2}{3}C_3)$, at 4665 G determining C_2 and at 7081 G determining C_3. Although the experiments at higher fields are probably more difficult, it seems reasonable to assert that $n = 2$ hydrogen and deuterium provide the opportunity to determine all six parameters of the model with roughly equal sensitivity, and therefore to test the detailed structure of the weak neutral currents involved.

IV. INVARIANT ANALYSIS OF MICROWAVE TRANSITION RATES

At the heart of any parity experiment is the measurement of the rate of some process in an apparatus which breaks inversion symmetry. The amplitude for any process can be separated into a parity conserving (PC) part and a parity nonconserving (PNC) part

$$R(\pm) = |A_{PC} \pm A_{PNC}|^2 = |A_{PC}|^2 + |A_{PNC}|^2 \pm (A_{PC}^* A_{PNC} + \text{c.c.}) .$$

$$(30)$$

The signs imply that reversing the sense of the handedness of the apparatus, by inversion of the symmetry breaking portions, will change the relative sign of these two amplitudes. Since $A_{PNC} \ll A_{PC}$ in atoms, we can drop $|A_{PNC}|^2$ and keep only the interference term. Its contribution will not appear in the mean rate R,

$$R \equiv \frac{1}{2}|R(+) + R(-)| \cong |A_{PC}|^2 ,$$

$$(31)$$

but will produce an asymmetry A in the rate,

$$A \equiv \frac{R(+) - R(-)}{R(+) + R(-)} \cong 2 \frac{|A_{PNC}|}{|A_{PC}|} \cos\phi .$$

$$(32)$$

Here ϕ is the relative phase of these two amplitudes, which changes $(\phi \to \phi + \pi)$ under reversal of the handedness of the apparatus. These formulas make it clear that a sensitive parity experiment will be possible if $|A_{PNC}|$ can be enhanced, $|A_{PC}|$ suppressed and if the handedness can be accurately reversed. Ideally, the decrease in the mean rate R arising from the suppression of $|A_{PC}|$ can be compensated by an increase in the number of atoms undergoing transitions. If it is possible to optimize all of these quantities, then a very weak PNC interaction can be "magnified" many times in the experiment, giving an asymmetry much larger than the parity mixture of the states.

There are important limitations to the size of the asymmetry and the sensitivity of the experiment. Assuming that $|A_{PC}|$ can be decreased by choice of the experimental parameters, the asymmetry will be increased ($A \propto |A_{PC}|^{-1}$) and the mean rate decreased ($R \propto |A_{PC}|^2$). It is generally advantageous to increase the asymmetry, since there are always competing systematics (false asymmetries). However, the signal-to-shot noise ratio (S/N) is independent of $|A_{PC}|$ and is not being improved in this way

$$S/N \propto AR/\sqrt{R} = 2|A_{PNC}| \cos\phi .$$

$$(33)$$

In practice, a suppression of the mean rate will always bring it into competition with some background rate. Further reduction of $|A_{PC}|$ would then begin to reduce S/N and decrease the sensitivity of the experiment. The optimum condition for the experiment is for R comparable to the background, and will result in an asymmetry and integration time determined by $|A_{PNC}|$ and

by background, but independent of $|A_{PC}|$. We have already seen this situation arise in the search for PNC in the $2S \to 1S + \gamma$ transition in hydrogen, for which the strongly suppressed $M1$ rate is much smaller than the background. We will see further examples in Sec. V.

The mean rate $R = |A_{PC}|^2$ is *even* under inversion of the sense of handedness of the apparatus, invariant under rotations, and is therefore expressible in terms of *scalar* combinations of the physical variables which appear in the rate. The asymmetry A is *odd* under inversions and expressible in terms of *pseudoscalar* combinations of the same variables. A simple listing of all possible scalars and pseudoscalars is a useful preliminary to the detailed design of a parity experiment. This invariant decomposition clarifies the alternative types of asymmetries and systematic corrections which can occur. This analysis requires only a knowledge of which variables will appear in the observed rate, and how many times they enter. We want to provide here an example of this analysis for parity experiments in $n = 2$ hydrogen.

In particle physics, it is generally the case that the only variables on the list are the momenta and spins of the incoming and outgoing particles, since the angular distributions are unaffected by external fields. In nuclear and atomic physics, many processes can be perturbed by electric and magnetic fields, which must then be added to the list. For $n = 2$ hydrogen, we have a new situation in which the states can be selected by static fields, and the transitions between them generated by microwave fields; thus *all* of the physical variables on our list are external fields. All of these fields can be controlled in strength, direction and relative phase, and this makes it possible to adjust the amplitudes for optimum sensitivity to weak interactions. In this situation there are pseudoscalar asymmetries which have not hitherto been used in parity experiments. This added degree of flexibility is a major advantage in hydrogen and provides strong motivation for working at microwave frequencies.

As proposed earlier it will be necessary to carry out hydrogen parity experiments with intense atomic beams.[2] Consider transitions between $2S$ states of hydrogen ($2S \to 2S'$) in a beam in a weak microwave field. In the presence of perturbations, these states will not have pure angular momentum and parity, but we will continue to refer to them as "S" states. They are distinguished from "P" states by their energy and by their narrow width. The microwave transitions under consideration will be weaker and have narrower line widths than the nearby $2S \to 2P$ transitions.

In the absence of perturbations, the $2S \to 2S'$ transitions have magnetic dipole amplitudes, generated by the interaction between an oscillatory magnetic field $\vec{b}$ and the intrinsic magnetic dipole moment

$$A_{PC}(M1) = -\vec{b} \cdot (2S'|\vec{\mu}|2S). \qquad (34)$$

If an electrostatic field $\vec{E}$ is present, then Stark mixing of $2S$ and $2P$ states occurs with amplitude

$$\delta_S \equiv \vec{E} \cdot \frac{(2P|e\vec{r}|2S)}{E(2S) - E(2P) + i\hbar\Gamma_{2P}/2}. \qquad (35)$$

This adds an electric dipole amplitude proportional to the oscillatory electric field $\vec{\epsilon}$,

$$A_{PC}(E1) = \delta_S\vec{\epsilon} \cdot (2S'|e\vec{r}|2P). \qquad (36)$$

There is an additional contribution to this amplitude from Stark mixing in the final state $2S'$, with the same form as Eq. (35). Although this perturbation mixes parity of the atomic states, it arises from PC terms in electrodynamics and is *even* under inversion of all the variables, if we remember to invert external as well as internal fields.

We must also include the weak mixing of $2S$ and $2P$ states with amplitude

$$\delta_W \equiv \frac{(2P|V_{PNC}|2S)}{E(2S) - E(2P) + i\hbar\Gamma_{2P}/2}, \qquad (37)$$

which adds a further PNC electric dipole amplitude

$$A_{PNC}(E1) = -\delta_W\vec{\epsilon} \cdot (2S'|e\vec{r}|2P). \qquad (38)$$

This amplitude is linear in the oscillatory field $\vec{\epsilon}$ but independent of the static field $\vec{E}$, and is odd under inversion.

For simplicity we restrict the discussion to these dipole amplitudes, neglecting higher multipoles and spatial variation of the external fields, since the wavelength $\lambda \simeq 20$ cm is much larger than the beam width $d \simeq 1$ cm. We also suppress amplitudes nonlinear in the microwave amplitude $\vec{\epsilon}, \vec{b}$ by choosing the microwave power low enough to give a small transition probability in one pass through the cavity. Under these conditions, adding the amplitudes and squaring will give a transition rate depending quadratically on $\vec{\epsilon}$, $\vec{b}$, and $\vec{E}$. The dependence on the static magnetic field will include all powers of $\vec{B}$, because we choose magnetic fields large enough to produce a level crossing. The energy denominators contain $\vec{B}$, and so the amplitudes and rates are nonlinear in $\vec{B}$.

The beam velocity is *not* included on our list of variables since it can be transformed to zero. We will understand the rates to be evaluated in the rest frame of the atom, and expressed in terms of the electromagnetic fields in that frame.

Only when we reexpress our formulas in terms of laboratory fields will the velocity appear explicitly. Also, we do *not* include on the list any "polarization tensors" describing the orientation of the spins in the beam. The atoms in the beam entering and leaving the microwave region will be prepared and detected in well defined hyperfine states which are fully resolved by the static magnetic field $\vec{B}$. The polarization of spins is therefore along $\vec{B}$, the alighment along $(B_i B_j - \frac{1}{3} B^2 \delta_{ij})$, etc.

The actual construction of the invariants is an elementary task once the list of variables is complete. Table II gives the scalars and pseudoscalars which can result from $A_{PC}(M1)$ and $A_{PNC}(E1)$, appropriate to parity experiments with no static electric field present. The scalars are quadratic in $\vec{b}$, and the pseudoscalars are bilinear in $\vec{\epsilon}$ and $\vec{b}$. Terms quadratic in $\vec{\epsilon}$, and in δ_W are dropped since they are unobservably small. We are using a complex representation for $\vec{\epsilon}, \vec{b}$ to include arbitrary phase relations between the two oscillatory fields. Since damping of the atomic states is significant during the transit time through the cavity, there is no simple phase relation between the dipole moments ($\vec{\mu}$) and ($e\vec{r}$), which are also assumed complex.

Table II shows that there are *six* pseudoscalars and a separate experimental configuration for each involving different orientations and phases of the microwave fields. Rotating fields can be used, for example, in the term $i(\vec{b} \times \vec{\epsilon}* \cdot \vec{B} - cc)$; oscillating fields with $\vec{\epsilon}$ and $\vec{b}$ in quadrature will also give a contribution for this term. This table displays the complete range of possibilities for microwave parity experiments with zero static electric field.

If, on the contrary, a similar analysis is carried out for an optical $M1$ transition, then it is necessary to restrict the fields $\vec{\epsilon}, \vec{b}$ to those of a real photon. This implies a relationship between their relative strength, orientation and phase given by $\vec{b} = \hat{k} \times \vec{\epsilon}$, where $\hat{k}$ is the propagation vector of the light ($\vec{\epsilon} \cdot \hat{k} = \vec{b} \cdot \hat{k} = 0$). In that case, there are *fewer* invariant combinations,

given in Table III.

These invariants are more familiar: the second scalar term is just the "Zeeman" term giving a (PC) circular polarization of the light emitted along the magnetic field. The first pseudoscalar term is the "*Wu*" term, giving the anisotropy of light emitted parallel or antiparallel to the magnetic field. The second pseudoscalar describes the intrinsic circular polarization of the light. Comparison of Tables II and III shows that some of the possible micorwave parity experiments have no optical analog.

It is of greater practical interest to consider instead the role of $A_{PC}(E1)$, the Stark-induced electric dipole amplitude. This amplitude can be adjusted to optimum size by changing the strength of E, and can be modulated for signal averaging to identify the interference term ($A_{PC}^* A_{PNC} + cc$). In Table IV we present the list of invariants arising from $|A_{PC}(E1) + A_{PNC}(E1)|^2$. To reduce the number of terms we have made the additional restriction that $\vec{\epsilon}$ is real, including linear but not circular polarization. We see that there are four separate pseudoscalar terms, and four configurations of the fields $\vec{\epsilon}$, $\vec{E}$, and $\vec{B}$ in which parity conservation can be tested. Since these terms result from the oscillatory electric field $\vec{\epsilon}$ alone, and are independent of the magnetic field $\vec{b}$, they each have an optical analog. Our earlier proposal[2] based on the circular dichroism of $2S \to 3S$ transitions does not appear on the list because of our elimination of rotating fields. In

TABLE II. Invariant terms in $|A_{PC}(M1) + A_{PNC}(E1)|^2$ for microwave transitions.

Scalars	Pseudoscalars
$\vec{b} \cdot \vec{b}*$	$(\vec{b} \cdot \vec{\epsilon}* + cc)$
$i(\vec{b} \times \vec{b}* \cdot \hat{B})$	$i(\vec{b} \cdot \vec{\epsilon}* - cc)$
$(\vec{b} \cdot \hat{B} \vec{b}* \cdot \hat{B})$	$(\vec{b} \times \vec{\epsilon}* \cdot \hat{B} + cc)$
	$i(\vec{b} \times \vec{\epsilon}* \cdot \hat{B} - cc)$
	$(\vec{b} \cdot \hat{B} \vec{\epsilon}* \cdot \hat{B} + cc)$
	$i(\vec{b} \cdot \hat{B} \vec{\epsilon}* \cdot \hat{B} - cc)$

TABLE III. Invariant terms in $|A_{PC}(M1) + A_{PNC}(E1)|^2$ for optical transitions.

Scalars	Pseudoscalars
$(\vec{\epsilon} \cdot \vec{\epsilon}*)$	$(\vec{\epsilon} \cdot \vec{\epsilon}*)(\hat{B} \cdot \hat{k})$
$i(\vec{\epsilon} \times \vec{\epsilon}* \cdot \hat{B})$	$i(\vec{\epsilon} \times \vec{\epsilon}* \cdot \hat{k})$
$(\vec{\epsilon} \times \hat{k} \cdot \hat{B})(\vec{\epsilon}* \times \hat{k} \cdot \hat{B})$	$(\vec{\epsilon} \times \hat{k} \cdot \hat{B})(\vec{\epsilon}* \cdot \hat{B}) + cc$
	$i[(\vec{\epsilon} \times \hat{k} \cdot \hat{B})(\vec{\epsilon}* \cdot \hat{B}) - cc]$

TABLE IV. Invariant terms in $|A_{PC}(E1) + A_{PNC}(E1)|^2$ for microwave transitions.

Scalars	Pseudoscalars
$\vec{\epsilon}^2 \vec{E}^2$	$\vec{\epsilon}^2 \vec{E} \cdot \hat{B}$
$(\vec{\epsilon} \cdot \vec{E})^2$	$(\vec{\epsilon} \cdot \vec{E})(\vec{\epsilon} \cdot \hat{B})$
$(\vec{\epsilon} \cdot \hat{B})^2 \vec{E}^2$	$(\vec{\epsilon} \cdot \vec{E} \times \hat{B})(\vec{\epsilon} \cdot \hat{B})$
$\epsilon^2(\vec{E} \cdot \hat{B})$	$(\vec{\epsilon} \cdot \hat{B})^2(\vec{E} \cdot \hat{B})$
$(\vec{\epsilon} \cdot \hat{B})^2(\vec{E} \cdot \hat{B})^2$	
$(\vec{\epsilon} \cdot \vec{E})(\vec{\epsilon} \cdot \hat{B})(\vec{E} \cdot \hat{B})$	
$(\vec{\epsilon} \cdot \vec{E} \times \hat{B})(\vec{E} \cdot \hat{B})$	
$(\vec{\epsilon} \cdot \vec{E} \times \hat{B})(\vec{\epsilon} \cdot \vec{E})$	

FIG. 6. Block diagram for metastable hydrogen beam apparatus.

the present notation it would correspond to the pseudoscalar terms $i(\vec{\epsilon} \times \vec{\epsilon}* \cdot \vec{E})$ and $i(\vec{\epsilon} \times \vec{\epsilon}*) \cdot (\vec{E} \times \vec{B})$.

It is clear from this discussion that the study of microwave transitions $2S \rightarrow 2S'$ in hydrogen offers the opportunity to measure the interference of parity conserving and parity nonconserving amplitudes under a wide variety of experimental configurations. The possibility of adjusting the amplitude A_{PC} to optimize the signal-to-noise ratio is undoubtedly a vital option in detecting the very small effects predicted by weak interaction theories. The use of Stark-induced electric dipole amplitudes is strongly suggested. In Sec. V we will consider in more detail one particular configuration illustrative of the realistic experimental situation.

V. SAMPLE MICROWAVE TRANSITION

The choice of a specific microwave transition to obtain the best sensitivity to weak interactions involves compromising many different requirements. In $n = 2$ hydrogen there are four $2S$ states and six possible transitions; the invariant analysis of Sec. IV showed that there were four different pseudoscalar combinations of fields. The final choice of the optimum configuration for an experiment must be made in the laboratory by empirical methods. Without trying to rationalize all the choices, we will analyze the rate for one specific example. This will clarify some of the techniques available for optimizing the sensitivity to parity nonconservation. Since it is clearly not feasible to directly measure an asymmetry as small as the parity mixture itself ($|\delta_W| \simeq 10^{-10}$), it is imperative to examine the means of suppressing A_{PC} and maximizing A_{PNC}.

The general arrangement for experiments with a beam of metastable hydrogen is shown in Fig. 6. An intense few hundred electron volts proton beam passes through a cesium vapor cell where resonant charge exchange takes place, producing a copious beam of $2S_{1/2}$ atoms ($\sim 10^{13}/cm^2 \sec$). This beam passes into a state selecting region in which a specific $2S$ state can be preferentially populated, and then into an interaction region in which microwave transitions between the metastable states $2S \rightarrow 2S'$ are induced. For a study of parity conservation, this interaction region should have a sense of handedness defined by one of the

pseudoscalars from Table IV. It is followed by a suitable detector to monitor the reappearance of the $2S'$ state.

The specific process to be considered is the transition $\alpha_0(2S, m_J = +\frac{1}{2}, m_I = -\frac{1}{2})$ to $\beta_0(2S, m_J = -\frac{1}{2}, m_I = +\frac{1}{2})$ in the vicinity of the first level crossing in the $n = 2$ shell (see Fig. 7). The microwave frequency is approximately 1600 MHz. The final state β_0 is chosen because it is the only state at this level crossing to be mixed with the nearby e states by weak interactions. The initial state α_0 is chosen because it has (predominantly) the opposite spin projections to β_0. This will help to suppress the parity conserving amplitude A_{PC} ($E1$), which is due to nuclear spin-independent interactions. This transition can be measured with very little background by depopulating both β states upstream from the microwave region, and by detecting their reappearance downstream. There are two stronger transitions $\alpha_{+1} \rightarrow \beta_0$ and $\alpha_0 \rightarrow \beta_{-1}$, and another weak transition $\alpha_{+1} \rightarrow \beta_{-1}$ nearby. All of these lines have very narrow width ($\lesssim 1$ MHz) governed by the transit time through the cavity, and by the Stark-induced width
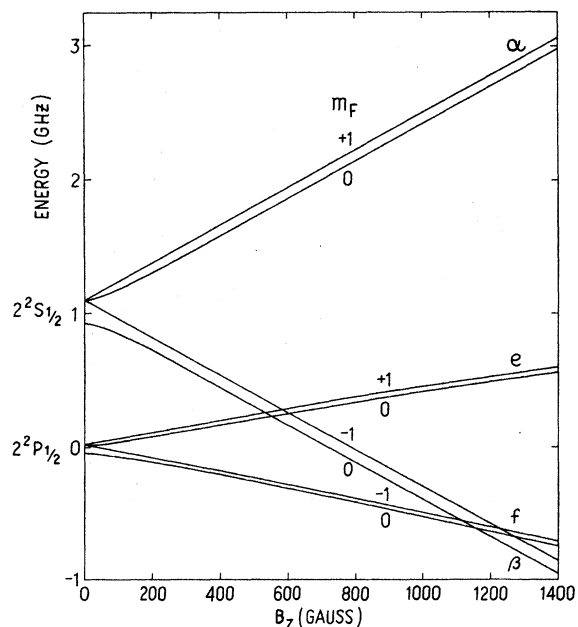
FIG. 7. Zeeman diagram for hydrogen at low fields, showing the hyperfine structure. The states are designated by the good quantum number m_F.
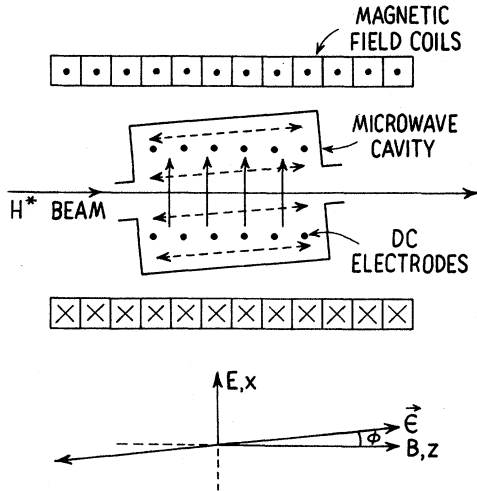
FIG. 8. Schematic diagram of interaction region for the microwave experiment.

of the β states

$$\Gamma_\beta = \Gamma_{2P} \frac{(\sqrt{3}\, ea_0 E_x)^2}{[E(2\beta) - E(2e)]^2 + (\hbar\Gamma_{2P}/2)^2}. \tag{39}$$

These four narrow lines are easily resolved. There is also a broad resonance $\alpha \to e$ overlapping these lines, which depopulates the metastable beam without contributing to the signal downstream. This resonance sets an upper limit to the microwave power.

A more detailed drawing of the interaction region is shown in Fig. 8, depicting a polarized beam passing through the microwave region. It consists of a solenoid which produces a static magnetic field along the beam axis. Inside the solenoid is a cylindrical microwave cavity operating in the lowest TM mode. This mode has an oscillatory electric field parallel to the axis of the cavity, but no such oscillatory magnetic field. The cavity axis is cocked at a small angle $\varphi \simeq 5°$ relative to the beam axis and to the static magnetic field. The cavity also contains appropriate wire grid electrodes to produce a static electric field $E_x \simeq 1$ V/cm, perpendicular to the magnetic field and in the plane defined by the cavity axis and the beam axis. The cavity can be tuned through the level crossing region ($\Delta f \approx 150$ MHz) and rotated about the magnetic field axis. With the magnetic field set near the β-e crossing, microwave transitions are driven from α_0 to β_0. The atoms produced in the β_0 state are relatively long lived in this weak electric field, enabling them to leave the cavity and enter the detector. In the detector, the β_0 states are selectively quenched as before and the resulting Lyman-α radiation is detected. The detector current is

a measure of the α_0 to β_0 transition probability, and is sensitive to the handedness of the interaction region if C_2 and/or C_3 are not zero.

In this configuration of fields, $\vec{E}$ and $\hat{B}$ are orthogonal and $\vec{\epsilon}$ is in the plane of $\vec{E}, \hat{B}$. Of the invariants from Table IV only one pseudoscalar and two independent scalar terms are nonvanishing, those proportional to $(\vec{\epsilon} \cdot \vec{E})^2$, $(\vec{\epsilon} \cdot \hat{B})^2 E^2$, $(\vec{\epsilon} \cdot \vec{E})(\vec{\epsilon} \cdot \hat{B})$. We are assuming perfect alignment of the directions of these fields and are neglecting the systematic corrections coming from misalignment errors and motional and stray fields. These can be also studied in detail using the invariant analysis. Choosing coordinates with $\hat{z}$ along $\hat{B}$ and $\hat{x}$ along $\vec{E}$, the axis of the cavity is in the (x, z) plane

$$\vec{\epsilon} = \epsilon(\hat{x}\sin\varphi + \hat{z}\cos\varphi), \tag{40}$$

and the rate contains three terms, proportional to

$$E_x^2 \epsilon_x^2, \quad E_x^2 \epsilon_z^2, \quad E_x \epsilon_x \epsilon_z. \tag{41}$$

The pseudoscalar term is odd under the reversal of E_x, of B_z and under rotation of the cavity through 180° about $z (\varphi \to -\varphi)$. The scalar terms are even under each of these operations. The presence of a small pseudoscalar term can therefore be discriminated from the much larger contributions of the scalar terms, by subtracting signals as each of these variables is reversed.

These properties of the signal can be traced to the handedness of the interaction region itself (see Fig. 8). Reflection of this apparatus in the x, z plane is equivalent to a reversal of the solenoid current alone, which reverses the magnetic field B_z but not the electric fields. Reflection in the x, y plane is equivalent to rotating the cavity through π about the z axis, which reverses the transverse oscillatory field ϵ_x alone. Inversion of all three coordinates is equivalent to reversing the polarity on the dc electrodes, which reverses the electrostatic field E_x alone. Since each of these operations can be accurately and independently carried out, the interaction region can be altered from right handed to left handed in three distinct ways. The reversal of E_x can be done on a millisecond time scale, suitable for electronic signal averaging, while the other two operations can only be done on a longer time scale.

The invariant decomposition given in Eq. (41) can be verified, and the coefficients evaluated, by a simple calculation[22] in which the Zeeman interaction is included in the unperturbed energy, but the Stark and weak interactions are treated as perturbations. The $1S_{1/2}, 2S_{1/2}$ states are considered as stable states, neglecting their decay in the interaction region. The $2P_{1/2}$ states are
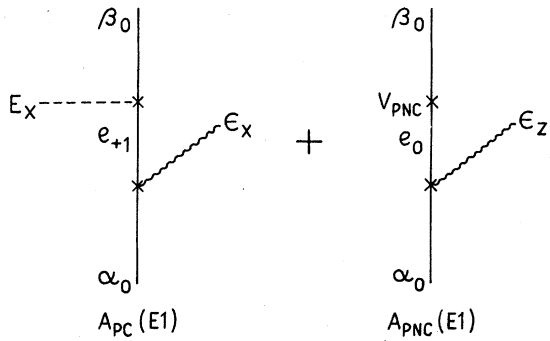
FIG. 9. Diagrams for the parity-conserving and parity-nonconserving electric dipole amplitudes in $\alpha_0 \to \beta_0$ transitions.

considered as virtual damped states; the $2P_{3/2}$ states are neglected. The relevant diagrams for $\alpha_0 \to \beta_0$ transitions are shown in Fig. 9, including only the lowest-order contributions. The matrix elements necessary to evaluate these amplitudes are

$$\langle e_{+1}|V_{\rm rf}|\alpha_0\rangle = \sqrt{3}\, ea_0 \epsilon_x \sin\theta\,,$$

$$\langle e_0|V_{\rm rf}|\alpha_0\rangle = \sqrt{3}\, ea_0 \epsilon_z \cos2\theta\,,$$

$$\langle \beta_0|V_{\rm static}|e_{+1}\rangle = \sqrt{3}\, ea_0 E_x \cos\theta\,,$$

$$\langle \beta_0|V_{\rm PNC}|e_0\rangle = 2i\bar{V}(C_{2p}+\tfrac{2}{3}C_{3p})\cos2\theta\,. \tag{42}$$

Here θ is the mixing parameter for different m_J, m_I components in states with given $m_F = m_J + m_I$ ($\theta \to 0$ in the Paschen-Back limit).

The amplitudes corresponding to these two diagrams are

$$A_{\rm PC} = \frac{3(ea_0)^2 \epsilon_x E_x \sin\theta\cos\theta}{E(\alpha_0) - E(e_{+1}) - \hbar\omega + i\hbar\Gamma_{2P}/2} \tag{43}$$

and

$$A_{\rm PNC} = (C_{2p}+\tfrac{2}{3}C_{3p})\frac{2i\sqrt{3}\, ea_0\bar{V}\cos^2 2\theta\epsilon_z}{E(\alpha_0) - E(e_0) - \tfrac{1}{2}\hbar\omega + i\hbar\Gamma_{2P}}\,. \tag{44}$$

The transition rate per atom is given by

$$R = (2\pi/\hbar)|A_{\rm PC}+A_{\rm PNC}|^2 \delta[E(\alpha_0) - E(\beta_0) - \hbar\omega]\,, \tag{45}$$

which contains a resonance of zero width at $\hbar\omega = E(\alpha_0) - E(\beta_0)$. This resonance will be broadened by damping and by the finite transit time, but the integrated rate will be independent of the width, and correctly given by integrating Eq. (45),

$$\hbar^2 \int R\,d\omega = 2\pi|A_{\rm PC}+A_{\rm PNC}|^2\,. \tag{46}$$

Examination of Eqs. (43)–(46) gives the following results: (i) The invariant decomposition in Eq.

(41) is verified, with one scalar term $|A_{\rm PC}|^2$ proportional to $\epsilon_x^2 E_x^2$ and one pseudoscalar term $(A_{\rm PC}A_{\rm PNC}^* + cc)$ proportional to $\epsilon_x \epsilon_z E_x$. The remaining scalar term, $\epsilon_z^2 E_x^2$, does not contribute to this particular transition because of angular momentum selection rules. Since the solenoid field has complete azimuthal symmetry, the unperturbed states have good $m_F = 0$. The weak interactions $V_{\rm PNC}$ and longitudinal electric field ϵ_z preserve m_F ($\Delta m_F = 0$); the transverse fields ϵ_x, E_x can generate an amplitude $A_{\rm PC}$ for $\alpha_0 \to e_{+1} \to \beta_0$ but the fields ϵ_z, E_x cannot. The weak interaction, together with the longitudinal field ϵ_z can generate an amplitude $A_{\rm PC}$ for $\alpha_0 \to e_0 \to \beta_0$, going through a different virtual state.

(ii) The amplitude $A_{\rm PC}$ is suppressed by two different factors. One factor (ϵ_x) can be reduced by making the angle φ small; for $\varphi \simeq \frac{1}{10}$ radian this reduces $A_{\rm PC}$ by one order of magnitude. The factor $\sin\theta$ expresses the small residual mixing of m_J, m_I states by the hyperfine interaction. At 575 G, the states α_0, β_0 have predominantly opposite spins, with a small admixture ($\sin\theta \simeq 0.06$) of parallel spins. Since electric dipole transitions preserve the proton spin, the amplitude $A_{\rm PC}$ is suppressed by this additional factor by more than one order of magnitude. There is no corresponding suppression of $A_{\rm PNC}$, which contains the "large" component of the rf electric field $\epsilon_z = \epsilon\cos\varphi$ and which contains weak interactions V_2, V_3 which can flip spins.

(iii) Since $A_{\rm PC}$ is linear in E_x and $A_{\rm PNC}$ is independent of E_x, the rate will be quadratic in E_x and the asymmetry will be inversely proportional to E_x. As we showed in Sec. IV, this leads to the possibility of increasing the asymmetry by reduction of E_x, with a corresponding loss of event rate and a constant ratio of signal-to-shot noise. The value of E_x should be chosen to make the shot noise comparable with other sources of noise in the apparatus. We can estimate typical running conditions by choosing $E_x \simeq 1$ V/cm, which implies an asymmetry on resonance

$$A = 2\left|\frac{A_{\rm PNC}}{A_{\rm PC}}\right| \simeq (C_{2p}+\tfrac{2}{3}C_{3p})\frac{4\bar{V}}{(\sqrt{3}\, ea_0 E_x)\varphi\,\theta}$$

$$= 4(C_{2p}+\tfrac{2}{3}C_{3p})\times10^{-6}\,. \tag{47}$$

This represents an enhancement of the intrinsic parity mixture by four orders of magnitude. To estimate the shot noise, we must also specify the microwave field strength, say $\epsilon \simeq 1$ V/cm. Then the integrated transition rate at resonance is

$$\int R\,d\omega \simeq 2\pi\left|\frac{3(ea_0)^2\epsilon E_x\varphi\,\theta}{\tfrac{1}{2}\hbar^2\Gamma_{2P}}\right|^2 \simeq 2\pi\times10^7 \ (\text{rad/sec})^2\,. \tag{48}$$

Taking the total transition line width as $(1/2\pi)\Gamma_I$ $\simeq 0.7$ MHz, this implies a counting rate at the center of the line, per atom,

$$\bar{R} = \frac{2}{\pi \Gamma_I} \int R d\omega \cong 10 \text{ rad/sec}. \tag{49}$$

Combining this with the incident flux $(J = 1 \times 10^{13} H^*/\text{sec})$, the flight time through the cavity $(\tau = 0.5 \ \mu\text{sec})$ and the efficiency of the detector $(\eta = 0.25)$, the event rate in the detector is

$$\mathcal{R} = \eta \bar{R} \tau J \approx 1 \times 10^7 \text{ sec}^{-1}. \tag{50}$$

This implies an integration time of approximately 2 h for $S/N = 1$ assuming $(C_{2p} + \frac{2}{3}C_{3p}) \simeq 1$. While these estimates are quite provisional, they clearly indicate the viability of microwave transitions as a means of detecting weak interactions in the hydrogen atom. Similar considerations for the β-f crossing give comparable sensitivity to $C_1 \pm (C_2 + \frac{2}{3}C_3)$ with integration times of several hours. The parity mixtures at the higher field crossings appear to be more difficult to measure, and have not yet been given serious consideration.

(iv) The contribution of different virtual states e_{+1}, e_0 in the two amplitudes leads to a variable phase difference between the two amplitudes, and a difference in line shape between the scalar and pseudoscalar terms. If we vary the magnetic field, while returning the microwave cavity to the center of the narrow resonance, then A_{PC} has a broad resonance $(\Delta B \simeq 52$ G) centered at the crossing of β_0 and e_{+1} $(B = 538$ G). The amplitude A_{PNC} has a resonance at the $\beta_0 - e_0$ crossing $(B = 553$ G). The scalar term $|A_{\text{PC}}|^2$ has a Lorentzian shape centered at 538 G; the pseudoscalar interference term $(A_{\text{PC}}^* A_{\text{PNC}}^* + \text{cc})$ has a resonance midway between the level crossings at 545 G, with a line shape which decreases faster than a Lorentzian in the wings. This magnetic line shape provides an important further criterion for recognizing the PNC term.

*Present address: Dept. of Physics, Princeton, N. J. 08540.

[1] H. Bethe and E. E. Salpeter, *Quantum Mechanics of One- and Two-Electron Atoms* (Springer, Berlin, 1957).

[2] R. R. Lewis and W. L. Williams, Phys. Lett. B **59**, 70 (1975); this letter will be referred to as I.

[3] Similar conclusions have been reached by E. A. Hinds and V. W. Hughes, Phys. Lett. B **67**, 487 (1977).

[4] M. A. Bouchiat and C. C. Bouchiat, Phys. Lett. B **48**, 111 (1974); A. N. Moskalev, Zh. Eksp. Teor. Fiz. Pis. Red. **19**, 229 (1974) [Sov. Phys. JETP Lett. **19**, 141, 216 (1974)]; I. B. Khriplovich Zh. Eksp. Teor. Fiz. Pis. Red. **20**, 689 (1974) [Sov. Phys. JETP Lett. **20**, 315 (1974)]; P. G. H. Sandars, *Atomic Physics* 4, edited by G. zu Putlitz, E. W. Weber, and A. Winnacker (Plenum, New York, 1975).

[5] Ya. B. Zel'dovich, Sov. Phys. JETP **9**, 682 (1959). The numerical values of the mixing amplitude was seriously overestimated in this paper.

[6] F. Curtis Michel, Phys. Rev. B **138**, 408 (1965).

[7] Wade L. Fite, R. T. Brackman, David G. Hummer, and R. F. Stebbings., Phys. Rev. **116**, 363 (1959).

[8] R. T. Robiscoe, Phys. Rev. **168**, 4 (1968).

[9] R. Marrus and R. W. Schmieder, Phys. Rev. A **5**, 1160 (1972). The $2S \rightarrow 1S$ transition has been observed in Tm by F. Boehm and A. Zehnder, Phys. Lett. B **59**, 440 (1975), setting a similar upper bound on δ. Since the $2S$-$2P$ states in this many-electron atom are not very close in energy, this experiment is somewhat beyond the scope of our concern here.

[10] G. Feinberg and M. Y. Chen, Phys. Rev. D **10**, 190 (1974).

[11] A. N. Moskalev, JETP Lett. **19**, 141 (1974); Ya. I. Aximov, A. A. Ansel'm, A. N. Moskalev, and R. M. Ryndin, Sov. Phys. JETP **40**, 8 (1975).

[12] It has been shown that radiative corrections to the electron-nucleon coupling constants are a few percent. These corrections can be absorbed into the coupling constants, and do not otherwise change our analysis. W. J. Marciano and A. I. Sanda (Rockefeller University, 1978) (unpublished); D. Touissant (Princeton University, 1978) (unpublished).

[13] C. Bouchiat, Phys. Lett. B **57**, 184 (1975); E. A. Hinds, C. A. Loving, and P. G. H. Sandars, Phys. Lett. B **62**, 97 (1976).

[14] J. Bernstein, *Elementary Particles and Their Currents* (Freeman, San Francisco, 1968).

[15] The existence of three distinct terms in this interaction has been recognized earlier in Refs. 10 and 11. The invariants formed from S, T, P couplings all lead to T-odd interactions and are excluded from our analysis. An intrinsic electric dipole moment of the electron or nucleon is another mechanism for breaking T- and P-invariance which we shall not consider.

[16] J. Bernabeu and C. Jarlskog, CERN Th 2206 (1976) (unpublished); S. J. Brodsky and G. Karl, SLAC 1625 (1975) (unpublished); R. N. Cahn and G. L. Kane, Phys.

Lett. B 71, 348 (1977).

[17]W. E. Lamb, Jr. and R. C. Retherford, Phys. Rev. 79, 549 (1950).

[18]The radial functions are given in Ref. 1; they are real and normalized to unity. The angular and spin parts given in Eq. (21) have the same phases and normalization as given by A. R. Edmonds, *Angular Momentum in Quantum Mechanics* (Princeton University, Princeton, N. J., 1960), Chap. 2.

[19]S. J. Brodsky and R. G. Parsons, Phys. Rev. 163, 134 (1967).

[20]F. D. Colegrove, P. A. Franken, R. R. Lewis, and R. H. Sands, Phys. Rev. Lett. 3, 420 (1959).

[21]We are excluding the consideration of parity experiments in the vicinity of "critically damped" states, in which both the real and imaginary parts of the energy difference goes through zero simultaneously. Lamb has shown that this can occur in $n=2$ hydrogen in a specific combination of electric and magnetic fields; see W. E. Lamb Jr., Phys. Rev. 85, 259 (1952). We have been unable to discover any way of using this phenomenon to advantage in the design of parity experiments.

[22]A more complete numerical analysis of the rates will be published soon.